Compression of Positron Clouds in the Independent Particle Regime

C. A. Isaac, C. J. Baker, T. Mortensen, D. P. van der Werf,* and M. Charlton

Department of Physics, College of Science, Swansea University, Singleton Park, Swansea SA2 8PP, United Kingdom

(Received 9 February 2011; published 12 July 2011)

The application of an asymmetric dipolar electric field rotating at a frequency close to that of the axial bounce of a collection of trapped positrons has, in the presence of a low pressure molecular gas to provide cooling, been used to achieve compression of the cloud. A theory of this effect has been developed for a Penning trap potential, with the cooling modeled in the Stokes viscous drag approximation. Good agreement between the theory and measurements of the frequency dependence of the cloud compression rate has been found, establishing that the phenomenon is a new form of sideband cooling.

DOI: 10.1103/PhysRevLett.107.033201 PACS numbers: 34.80.Uv, 37.10.De, 37.10.Ty, 52.27.Jt

Low energy positrons have found major applications over the years, mainly as probes in the fields of atomic and condensed matter physics (see, e.g., [1,2]). Recent innovations have involved the accumulation and control of clouds of the antiparticles, often in the form of single component plasmas [3], and their uses in the formation and trapping of cold antihydrogen [4–6], the creation of systems containing more than one positronium atom [7], and scattering and annihilation studies at unprecedented energy resolutions (see, e.g., [8]).

The positron plasmas are typically held in a Penning-type trap (see below) and their radial extent can be controlled by applying a time-varying dipolar or quadrupolar electric field which rotates in the same sense as the natural plasma rotation in the combined electric and magnetic fields of the system. It has been found that this rotating wall technique, which was first developed for ions [9] and electrons [10], can be applied over a broad range of frequencies to electron and positron plasmas in a so-called strong drive regime in which the final density of the plasma is fixed by the applied frequency [11,12]. To counteract heating of the plasma by the rotating wall, cooling is provided by added gases or, if a high magnetic field trap is used, by the emission of cyclotron radiation.

For single particles, or clouds in the independent particle regime, held in Penning traps, several groups, following Wineland and Dehmelt [13], have used sideband excitation to axialize charged particles. This has been achieved in conjunction with a number of cooling techniques, with their application dependent upon the species and experimental circumstances [14–16]. Recently, antiprotons have been sideband cooled using electrons as a ''non-neutral buffer gas'' [17]. In all these cases the sidebands were excited by adding to the static trap fields an oscillating azimuthal quadrupolar electric field which varied in time as $\cos(\omega t)$, where ω is close to one of the natural frequencies of the system.

Although the rotating wall technique was believed to be applicable only to plasmas, it has recently been shown to produce positron cloud compression in the independent particle limit [18,19]. It was observed that the highest central density occurred close to the characteristic axial bounce frequency. A number of possible compression mechanisms were discussed including excitation of plasma modes, magnetron sideband cooling, and bounce resonance transport, and it was tentatively concluded that the last effect was the likely cause of the phenomenon.

The importance of the observation of cloud manipulation outside the plasma regime is that the effect can be used to dramatically improve the quality and control of positron beams and be applied using, as here, a two-stage accumulator [20] which is a relatively modest addition to current technologies. In this Letter we describe a study of the behavior of the compression rate and associated parameters as the frequency and amplitude of the applied rotating wall voltage, and the gas pressure, are varied. We also develop a theory of the effect which compares favorably with experiment. It will be shown, contrary to previous conjecture [19], that the compression occurs as a result of a new mode of motional sideband cooling.

A Penning-type trap typically consists of a number of cylindrically symmetric electrodes used to produce a potential extremum which in conjunction with a magnetic field, $\mathbf{B} = B\hat{\mathbf{z}}$, applied parallel to the symmetry axis can provide confinement of charged particles. The ideal electrical potential experienced by a charged particle in such a trap is given by the first term of the following equation:

$$\phi(z, r, \theta) = \frac{m}{q}\frac{\omega_z^2}{2}\left(z^2 - \frac{r^2}{2}\right) + \frac{m}{q}azr\cos(\theta + \omega_r t). \quad (1)$$

The value of the axial bounce frequency, ω_z, depends on the electrode geometry and the applied voltages. In a constant magnetic field and zero perpendicular electric field, charged particles orbit the field axis at the cyclotron frequency, $\Omega_c = qB/m$, where q and m are the charge and the mass of the particle, respectively. The application of a Penning trap potential also gives rise to crossed $\mathbf{E} \times \mathbf{B}$ fields which modify Ω_c into ω_+, and cause the particle to exhibit magnetron motion with a frequency ω_-. The latter

frequencies are given by $\omega_\pm = \frac{1}{2}(\Omega_c \pm \sqrt{\Omega_c^2 - 2\omega_z^2})$. For the parameters used in our experiment $\omega_+ \approx 4.40\ \mathrm{Grad\,s^{-1}}$, $\omega_z \approx 59.6\ \mathrm{Mrad\,s^{-1}}$, and $\omega_- \approx 399\ \mathrm{krad\,s^{-1}}$.

Adding an asymmetric rotating wall potential, with angular frequency ω_r and where a is proportional to the amplitude of the voltage, can be represented by the second term in (1). Assuming the cooling (which is a result of inelastic collisions with an added gas molecule; see below) can be described by a Stokes viscous drag term with friction coefficient, κ, the equations of motion for a trapped particle become

$$\begin{aligned}\ddot{x} &= \frac{\omega_z^2}{2}x - az\cos(\omega_r t) + \Omega_c\dot{y} - \kappa\dot{x},\\ \ddot{y} &= \frac{\omega_z^2}{2}y + az\sin(\omega_r t) - \Omega_c\dot{x} - \kappa\dot{y},\\ \ddot{z} &= -\omega_z^2 z - a[x\cos(\omega_r t) - y\sin(\omega_r t)] - \kappa\dot{z}.\end{aligned} \tag{2}$$

Following the approach of Brown and Gabrielse [14], the equations of motion (2) can be expressed in a new coordinate system defined by $\mathbf{V}^\pm = \dot{\mathbf{r}} + \omega_\mp \hat{\mathbf{z}} \times \mathbf{r}$, which decouples the magnetron ($-$) and cyclotron ($+$) motions as

$$\dot{V}_x^\pm = \omega_\pm V_y^\pm - \kappa\left[V_x^\pm + \frac{\omega_\mp}{\omega_+ - \omega_-}(V_x^+ - V_x^-)\right] - az\cos(\omega_r t), \tag{3a}$$

$$\dot{V}_y^\pm = -\omega_\pm V_x^\pm - \kappa\left[V_y^\pm + \frac{\omega_\mp}{\omega_+ - \omega_-}(V_y^+ - V_y^-)\right] + az\sin(\omega_r t), \tag{3b}$$

$$\ddot{z} = -\omega_z^2 z - \kappa\dot{z} - \frac{a}{\omega_+ - \omega_-}[(V_y^- - V_y^+)\cos(\omega_r t) - (V_x^+ - V_x^-)\sin(\omega_r t)]. \tag{3c}$$

Since the applied rotating wall frequency, which as will be shown below is centered around $(\omega_z + \omega_-)$, is far from the cyclotron frequency, the latter motion is effectively decoupled and only the terms containing the magnetron behavior need to be retained [14]. Furthermore, because the friction in the axial direction is much larger than that experienced by the magnetron motion (since $\omega_-/\omega_+ \ll 1$), the friction terms in (3a) and (3b) can be neglected to leave

$$\begin{aligned}\dot{V}_x^- &= \omega_- V_y^- - az\cos(\omega_r t),\\ \dot{V}_y^- &= -\omega_- V_x^- + az\sin(\omega_r t),\\ \ddot{z} &= -\omega_z^2 z - \kappa\dot{z} - a\frac{[V_y^-\cos(\omega_r t) + V_x^-\sin(\omega_r t)]}{\omega_+ - \omega_-}.\end{aligned} \tag{4}$$

These equations have been solved analytically to reveal that the particles exponentially approach the symmetry axis with a characteristic compression rate, Γ, given by

$$\Gamma = \frac{\kappa}{4}\left(1 - \sqrt{\frac{(\omega_r - \omega_0)^2}{\delta^2 + (\omega_r - \omega_0)^2}}\right), \tag{5}$$

where $\omega_0 = \omega_z + \omega_-$ and the width, δ, is dependent on the applied rotating wall amplitude via

$$\delta = \frac{a}{\sqrt{(\omega_+ - \omega_-)\omega_z}}. \tag{6}$$

Our compression experiments were performed in a two-stage positron accumulator which uses collisions with nitrogen buffer gas (at a pressure around 6×10^{-4} mbar) to promote capture of the positrons from a low energy beam [20]. Cooling was achieved using SF_6 gas [18,21] which was admitted at various pressures to the chamber near the second stage of the accumulator.

A series of cylindrical electrodes in the second stage (see Fig. 1) was used to produce a trapping potential. The rotating wall electric field was provided by splitting one of the 49 mm long electrodes into two, with one of the halves segmented azimuthally into four parts. The rotating wall potentials were created by a synthesizer arrangement to produce a phase difference of $\pi/2$ between successive segments.

For the present studies, about 10^4 positrons were captured in 100 ms, whereupon accumulation was halted and the rotating wall switched on for a time, t_c, before the cloud was ejected. The radius of the cloud was extracted using a technique which allowed measurements to be taken rapidly as the frequency of the rotating wall was varied. The method utilizes the observation that for a thermal cloud in the single particle limit, the magnetron radii have a Gaussian distribution. As such, the radial profile of a dumped cloud is Gaussian, provided (as is the case here) the cyclotron orbit is small with respect to that of the magnetron motion. The Gaussian profile was validated in separate experiments using images from a phosphor screen arrangement.

The system is shown schematically in Fig. 1 and illustrates how the ejected cloud must interact with two plates inserted into its path. Plate 1 has a hole on the axis of the

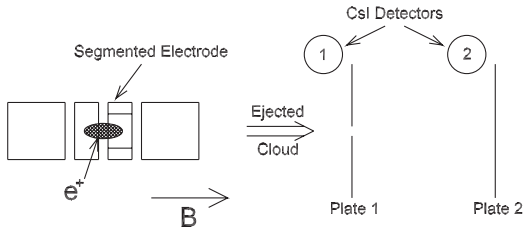

FIG. 1. Schematic of the accumulator second stage with a segmented electrode and the plate system used to measure the radius of the ejected positron cloud.

beam line of radius $r_0 = 1$ mm such that those positrons, numbered N_1, with trajectories of radii larger than this annihilate on the plate. The remainder, N_2, pass through and annihilate on the second plate. The resultant gamma rays are detected by calibrated CsI scintillator-photodiode arrangements, to provide values for N_1 and N_2. It can be shown that the width, σ, of the Gaussian profile can be derived using the signals from the detectors as

$$\sigma = \frac{r_0}{\sqrt{2\ln(1 + N_2/N_1)}}. \quad (7)$$

The inset in Fig. 2 shows the results of a typical sequence of measurements of the cloud radius (defined as σ) as a function of t_c. Though it is expected (see above) that for long times the radius will tend to zero, it is apparent that the cloud approaches a minimum size. By assuming the cloud experiences a constant expansion rate, γ, the data were fitted using $\sigma(t) = (\sigma_0 - \gamma/\Gamma)\exp(-\Gamma t) + \gamma/\Gamma$, where σ_0 is the width of the cloud before application of the rotating wall. The origin of γ is not yet understood, but it is likely to be related to collisions with the buffer and cooling gases and the presence of trap field asymmetries, both of which are known to cause cloud expansion, at least in the plasma regime [22,23].

By measuring the compression rate as a function of rotating wall frequency and amplitude, Eqs. (5) and (6) can be tested. In Fig. 2 the compression rate is plotted versus frequency for three rotating wall amplitudes. The solid line shows the fit to the data using Eq. (5) and displays very good agreement. Measurements were performed for amplitudes up to 0.6 V, and the derived values for δ are plotted in Fig. 3. The data are fitted well by the straight line, as expected from Eq. (6), but with an offset (see below). It can be shown from Eq. (1) that the rotating wall peak-to-peak voltage, V_r, is given by $(m/q)af$, where f is a geometrical trap factor. This can be estimated by approximating the electrical potential in the trap using two first order (in r and z) Taylor expansions to yield a value of ~ 61 kHz V^{-1} for comparison with the fitted gradient in Fig. 3.

The offset and higher than expected gradient present in the data in Fig. 3 may be attributed to the anharmonicity of the well used. Numerically evaluating the distribution of bounce frequencies of the trap for a cloud temperature of ~ 55 meV, and subsequently convoluting the results with Eq. (5), produces a frequency response consistent with the observed offset, without significantly distorting the profile. If a linear relationship between the cloud temperature and rotating wall drive amplitude is assumed, then the resulting broadening of the response width increases the gradient of the data in Fig. 3 when compared with the prediction of Eq. (6). A temperature increase of around 10 meV per volt applied is sufficient to account for the difference.

Figure 4 shows the friction coefficient, κ, versus SF_6 pressure for two different rotating wall amplitudes, indicating a linear relationship characteristic of a viscous friction model. We note, though, that this result may not be generally valid as the temperature of the positrons will depend upon the gas pressure and the drive amplitude via the cross section for the scattering process responsible for cooling [8]. The offset in Fig. 4 is likely a result of this interplay. Below a certain SF_6 pressure the cooling is insufficient to prevent energy gain of the positrons which results in their loss from the trap, likely as a result of positronium formation.

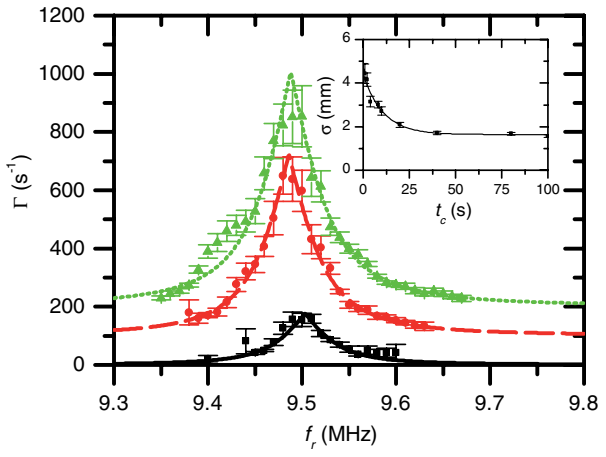

FIG. 2 (color online). Compression rate as a function of the rotating wall frequency for amplitudes of 75 mV (■), 150 mV (●), offset by 100 s^{-1} and 225 mV (▲), offset by 200 s^{-1}. The line is fitted using Eq. (5). Inset: Ejected cloud radius versus the rotating wall on-time; the line is a fit to $\sigma(t)$ (see text). The uncertainties on the points in both graphs are due to scatter on repeated measurements.

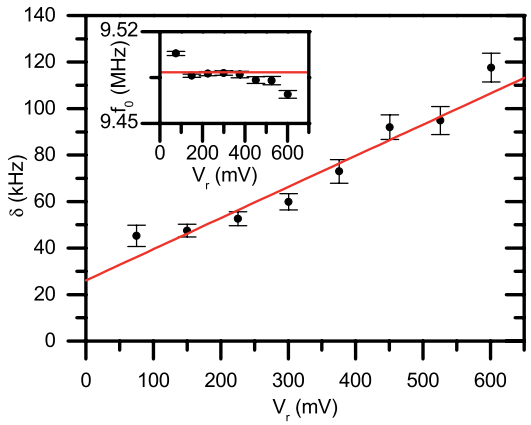

FIG. 3 (color online). Frequency response width versus the applied rotating wall amplitude with a fitted gradient of 134 ± 15 kHz V^{-1} and an offset of 26.1 ± 4.5 kHz. The inset shows that the central frequency of the response curve remains more or less constant across this range of amplitudes with a mean value of 9.4889 ± 0.0030 MHz, which is in excellent agreement with the calculated value of 9.49 MHz from the parameters given in the text. The uncertainties are derived from the fits to Eqs. (5) and (6).

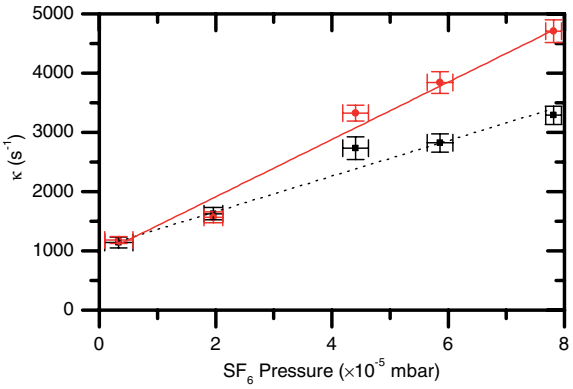

FIG. 4 (color online). Friction coefficient, κ, versus SF_6 pressure for rotating wall amplitudes 150 mV (■) and 225 mV (●).

It is notable that the values of κ vary with the amplitude of the rotating wall voltage. This is probably caused by the shortcomings of the Stokes description of the cooling, since the vibrational excitation collisions involved are known to be strongly energy dependent at low energies [8]. However, for rotating wall amplitudes in the range 0.06–0.60 V we find values of κ spanning 500–5000 s^{-1}. We can compare this to the cooling time of 0.36 s measured at a pressure of 2×10^{-8} mbar under similar circumstances [21]. At 1×10^{-5} mbar this implies a cooling rate of $\sim$1400 s^{-1}, in acceptable accord with the values extracted above.

Aspects of our approach can be compared to that in Ref. [19]. However, care must be exercised when doing so, since their results were presented in the form of a central density parameter, a measure which masks the underlying variables of frequency response width and compression rate by convoluting the width and total number of particles present, both of which may simultaneously vary. By extracting a central density from our data we observe similar trends to [19] in the variation of the frequency response width (broadening and asymmetry) and central frequency position (shifts) as V_r is varied. However, only qualitative comparisons are possible.

We have shown rotating wall compression of a cloud of positrons in the independent particle regime and, from theory developed here, that it is a new form of sideband cooling due to the use of an asymmetric dipolar rotating field. An important aspect of this technique is that, in contrast to the oscillating excitations which have mostly been used previously, the rotating nature of the field means that only one sideband (near the axial bounce frequency) is active. This removes the need for the use of narrow resonances to achieve sideband cooling and makes the methodology applicable to a variety of useful trap or accumulator geometries and to produce higher brightness positron beams. We note that the width of the response curve has a weak dependence upon q/m as $\delta \propto (q/m)^{1/4}$, which should render this technique applicable to a wide variety of species.

We are grateful to Dr. Rod Greaves of First Point Scientific Inc. for numerous helpful discussions. We thank the EPSRC for its support of our program, currently via EP/E048951/1 and EP/H026932/1. We thank S. J. Kerrigan and P. R. Watkeys for their help with earlier experiments and the technical staff of the Physics Department for their enthusiastic support. D. P. v. d. W. is grateful to RCUK.

*Corresponding author.
D.P.van.der.Werf@Swansea.ac.uk

[1] M. Charlton and J. W. Humberston, *Positron Physics* (Cambridge University Press, Cambridge, England, 2001).
[2] *Positron Beams and Their Applications*, edited by P. Coleman (World Scientific, Singapore, 1999).
[3] L. V. Jørgensen *et al.*, Phys. Rev. Lett. **95**, 025002 (2005).
[4] M. Amoretti *et al.*, Nature (London) **419**, 456 (2002).
[5] G. Gabrielse *et al.*, Phys. Rev. Lett. **89**, 213401 (2002).
[6] G. B. Andresen *et al.*, Nature (London) **468**, 673 (2010).
[7] D. B. Cassidy and A. P. Mills, Jr., Nature (London) **449**, 195 (2007).
[8] C. M. Surko, G. F. Gribakin, and S. J. Buckman, J. Phys. B **38**, R57 (2005).
[9] X. P. Huang, F. Anderegg, E. M. Hollmann, C. F. Driscoll, and T. M. O'Neil, Phys. Rev. Lett. **78**, 875 (1997).
[10] F. Anderegg, E. M. Hollmann, and C. F. Driscoll, Phys. Rev. Lett. **81**, 4875 (1998).
[11] J. R. Danielson and C. M. Surko, Phys. Rev. Lett. **94**, 035001 (2005).
[12] J. R. Danielson, C. M. Surko, and T. M. O'Neil, Phys. Rev. Lett. **99**, 135005 (2007).
[13] D. Wineland and H. Dehmelt, Int. J. Mass Spectrom. Ion Phys. **16**, 338 (1975); **19**, 251 (1976).
[14] L. S. Brown and G. Gabrielse, Rev. Mod. Phys. **58**, 233 (1986).
[15] G. Savard *et al.*, Phys. Lett. A **158**, 247 (1991).
[16] H. F. Powell, D. M. Segal, and R. C. Thompson, Phys. Rev. Lett. **89**, 093003 (2002).
[17] A. Kellerbauer *et al.*, Phys. Rev. A **73**, 062508 (2006).
[18] D. B. Cassidy, S. H. M. Deng, R. G. Greaves, and A. P. Mills, Jr, Rev. Sci. Instrum. **77**, 073 106 (2006).
[19] R. G. Greaves and J. M. Moxom, Phys. Plasmas **15**, 072 304 (2008).
[20] J. Clarke *et al.*, Rev. Sci. Instrum. **77**, 063 302 (2006).
[21] R. G. Greaves and C. M. Surko, Phys. Rev. Lett. **85**, 1883 (2000).
[22] J. H. Malmberg and C. F. Driscoll, Phys. Rev. Lett. **44**, 654 (1980).
[23] J. Notte and J. Fajans, Phys. Plasmas **1**, 1123 (1994).